

Neutron defect emulation using ion beam in zircaloy-4

Mahmoud Izerrouken^{a*}, Omar Menchi^a, Yasmine Bouzemboua^b, Amal Maddouri^b, Sana Bouzidi^c

^aNuclear research center of Draria, Bp. 43, Sebbala street, Daria, Algiers, Algeria; m-izerrouken@crnd.dz

^bAbderrahman Mira University Bejaia, Algeria

^cFaculty of physics, USTHB, Algiers, Algeria

* Corresponding author. M-izerrouken@crnd.dz

Article history: 20 July 2024, Revised 06 October 2024, Accepted 20 October 2024

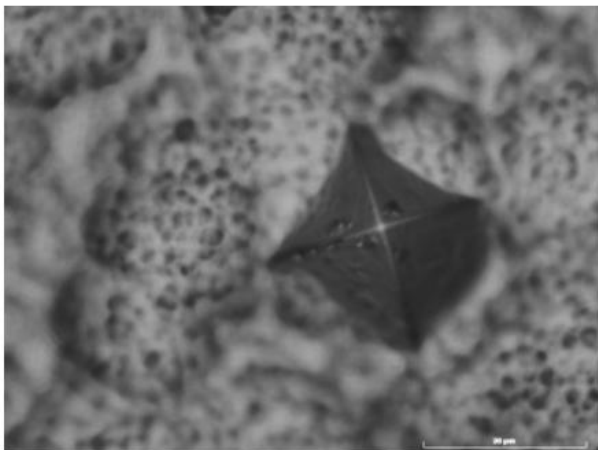
ABSTRACT

The present study is devoted to study ion beam induced defects in zircaloy-4. We focused on the effect on the surface morphology modifications. The samples are first polished and then bombarded with 20 MeV Au ion and 0.7 MeV Cu ion at room temperature to a dose of 4.5 dpa. After irradiation the samples were subjected to chemical etching in 47 ml nitric acid (HNO₃), 3 ml hydrofluoric acid (HF) and 50 ml water (H₂O). Optical microscopy observation showed drastic changes in the microstructure after irradiation. The observation at the interface between the irradiated part and non-irradiated part revealed a clear shrinkage parallel to the ion beam direction. Fine grain of about 10 μm diameter are formed on the surface of zircaloy-4 irradiated at low energy ($S_n/S_e \ll 1$) while a hillocks-like nanostructure is observed in the case of high energy irradiation ($S_n/S_e \gg 1$). Both cases can affect the zircaloy-4 corrosion resistance.

Keywords: Radiation damage; Irradiation growth; Reactor neutron; Zircaloy-4; Craters; structural components; fuel cladding.

Graphical abstract

Ion beam irradiation induced a nanostructure causing hardening of Zircaloy-4 and affecting its corrosion resistance.



Recommended Citation

Izerrouken M, Menchi O, Bouzemboua Y, Maddouri A, Bouzidi S. Neutron defect emulation using ion beam in zircaloy-4. *Alger. J. Eng. Technol.* 2024, 9(2): 138-143., <http://dx.doi.org/10.57056/ajet.v9i2.174>

1. Introduction

Simulation of neutron damage by ion beam irradiation is a commonly used method to study radiation damage in structural materials [1]. Neutron irradiation requires a long time due to the very low damage rate of 1×10^{-7} atomic displacement. s^{-1} in addition to the high radioactivity generated, which requires hot cells for sample handling. whereas ion beam irradiation induces a much higher displacement rate 1×10^{-5} displacement. s^{-1} , lower radioactivity and offers the possibility of controlling the irradiation parameters (flux, fluence, temperature pressure, ...). Thus, ion beam irradiation becomes an effective solution to study radiation damage and understand the mechanism of defects in structural materials.

Zirconium-based alloys (zircaloy-2, zircaloy-4 and Zr-2.5%Nb) are widely used in nuclear technology as fuel cladding material in pressurized water reactors (PWRs), boiling water (REB) and research reactors. They are also used for long-term storage of nuclear waste [2]. Furthermore, given the demand for energy and the need for radioisotopes for medicine, it has become necessary to extend the life of operating reactors. Thus, very extensive studies have been carried out to prove the resistance to radiation damage of current structural materials at higher doses [3].

Among the most important characteristics of zircaloy for nuclear applications, besides its low thermal neutron absorption cross section, is the absence of swelling by irradiation. After irradiation, zircaloy can experience irradiation growth, a process by which it expands in the direction of the a-axis but shrinks along the c-axis. A dimensional change at a constant volume known also as no swelling process. This process remain poorly understood [4]. Since the observation of this phenomenon in zircaloy [5], several theoretical and experimental research works have been carried out in order to clarify the causes responsible for this process [6-10]. Several models of irradiation growth irradiation growth were discussed in ref. [11]. In their model, authors simulated the irradiation growth based on the evolution of point defects and interstitial dislocation loops, induced by fast neutrons, and found good agreement with the experimental data. R. Adamson et al. [4] mentioned that irradiation growth is influenced by the microstructure, mainly grain size, degree of cold-working and dislocation density. Ion irradiation can be helpful to study this phenomenon. However, we note also ion beam irradiation induced crater and nanostructure at the surface of metals. The latter may considerably affect the corrosion resistance of nuclear reactor components. Given its importance for nuclear applications, this process is also well studied in several articles see ref. [12] and references therein. In the present paper, we focus on the surface morphology evolution under irradiation.

2. Materials and Methods

The material investigated in this work is zircaloy-4 with a thickness of about 2 mm. The chemical composition of the alloy is 1.6 wt% Sn, 0.21 wt% Fe, 0.08 wt% Cr, 0.1 wt% O, 0.29 wt% (Fe+Cr) and 97.7 wt% Zr. Small pieces of sizes about 10mm×10 mm, were cut from the same zircaloy-4 plate with a diamond saw and then grounded up to grade 1200 SiC sandpaper, followed by polishing with 3 μ m alumina suspensions. Before each irradiation the samples were cleaned with alcohol. The samples were irradiated with by 700 keV Cu and 20 MeV Au ions at room temperature in a vacuum chamber at 3×10^{-7} torr and the current was maintained at a constant current of 100 nA. During irradiation, the samples were partially masked in order to make a direct comparison between the irradiated and non-irradiated part. The irradiations were performed at National Center of Physics, Islamabad, Pakistan using 5UDH-2 Pelletron Tandem accelerator. The ion range R_p , electronic stopping power S_e , nuclear stopping power S_n , were obtained from SRIM2003 [13]. The irradiation fluence and dose are summarized in table 1.

The conversion from fluence to dose was made using equation (1) [14].

$$dpa = \frac{\phi N_d A}{\rho d N_A} \quad (1)$$

where ϕ is the Cu ion fluence, N_d is the number of displacements per ion, A is the molecular mass of the target material, ρ is the density, d is the penetration depth, N_A is Avogadro's number. The displacement damage $\left(\frac{N_d}{d}\right)$ was calculated using SRIM 2003 code with displacement energy threshold of 40 eV and using the "quick cascade calculation" (see Fig. 1). The doses (dpa) reported in table 2 are calculated at the peak damage.

Table 1: Irradiation parameters

Ion species	Energy (MeV)	S_e (keV/nm)	S_n (keV/nm)	Range (μm)	Fluence (ions. cm^{-2})	Dose (dpa)
Cu	0.7	0.68	0.89	0.32	1×10^{15}	2.3
Au	20	5.24	1.57	2.86	1×10^{15}	4.5

The microstructure examination was then performed using chemical etching associated with the ZEISS microscope. The revelation of the grain boundary was carried out in a solution composed of 47 ml nitric acid (HNO_3), 3 ml hydrofluoric acid (HF) and 50 ml water (H_2O). Micro-hardness tests were performed using micro-durometer INOVASTEST. The measurements were carried out at room temperature using a Vickers indenter with loads of 100 gf and load times of 10 s.

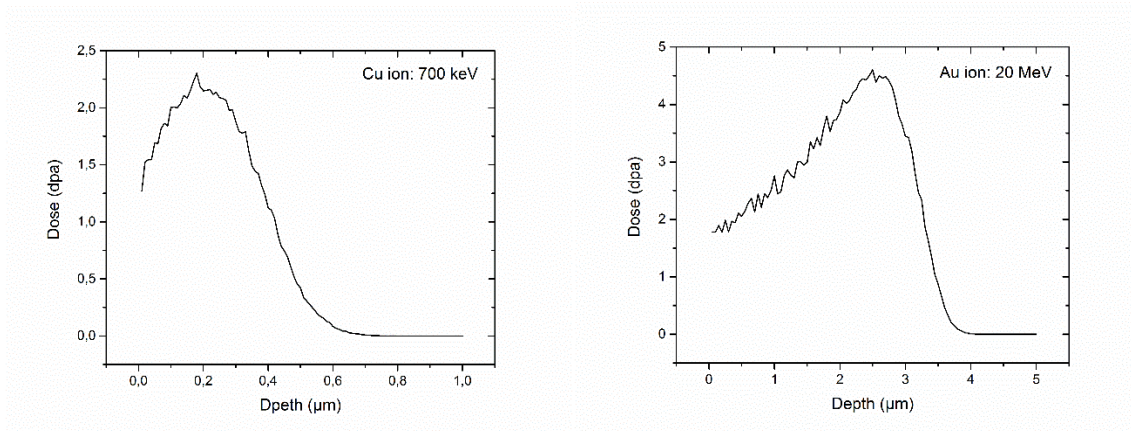


Fig. 1: displacement damage in zircaloy-4 induced by 700 keV Cu ion and 20 Au ion

3. Results and Discussion

Figure 2 reports the image of zircaloy-4 before chemical etching indicating a clear demarcation between the irradiated and non-irradiated parts. The irradiated part appears very damaged; grains and grain boundaries are indistinguishable. After chemical etching (see Fig. 3), the image reveals a clear surface morphology modification compared to the non-irradiated part. Indeed, the solution attacked preferentially the irradiated region. These zones are mainly grain boundaries and defects which are considered sinks for vacancy and interstices. During irradiation the vacancies and interstices migrate towards grain boundaries and dislocation causing drastic microstructure modification. In addition, observations of the interface between the irradiated part and the non-irradiated parts, revealed a clear shrinkage in the ion beam direction (perpendicular to the irradiated surface). The thickness of the irradiated part is reduced compared to the non-irradiated part. Thought, this could come also from the etchant having removed more material in the irradiated area. So, more investigation using electron backscatter diffraction (EBSD) before and after irradiation is needed to confirm the correlation between irradiation growth and microstructural evolution, as revealed in previous results [15].

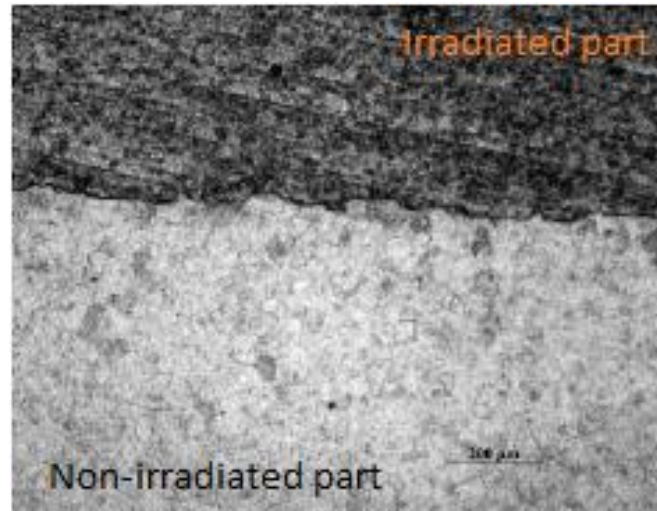


Fig. 2: Optical microscopy micrograph showing irradiated and non-irradiated of cold-worked zircaloy.

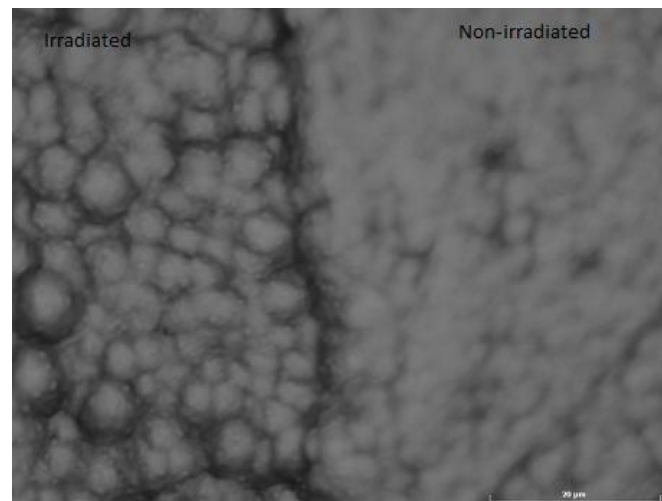


Fig. 3: Optical microscopy micrograph of sample irradiated with 700 keV Cu ion at 2.4 dpa observed after chemical etching showing refined grain or sub-grain structure .

Figure 4 a and b and c show respectively the surface microstructure observed after 700 keV Cu ion and 20 MeV Au ion irradiation. One can see the formation of homogeneous fine grains with equiaxed shape of about 5 – 10 μm diameter in the case of 700 keV Cu ion irradiation whereas the surface morphology of the sample irradiated with 20 MeV Au ion revealed hillocks-like nanostructure formation. This difference may be attributed to the ion beam interaction mechanism. Cu ion of 700 keV with S_n/S_e ratio of 1.3 interact mainly via elastic collision with target nuclei generating cascades of atomic displacements. The vacancies may form vacancy clusters and dislocation loops which explain the formation of small circular grain. However, in the case of 20 MeV Au ion irradiation, the electronic ionization and excitation ($S_n/S_e = 0.3$) are the main energy loss process, with the formation of ion tracks. This energy deposition produces extreme heat along the ion's path. This results in the ejection of material from the inner layers towards the surface forming nanostructures. It should be noted that some features look like craters but it is hard to tell because it is a top view picture. So profilometry analysis is useful to confirm the craters formation.

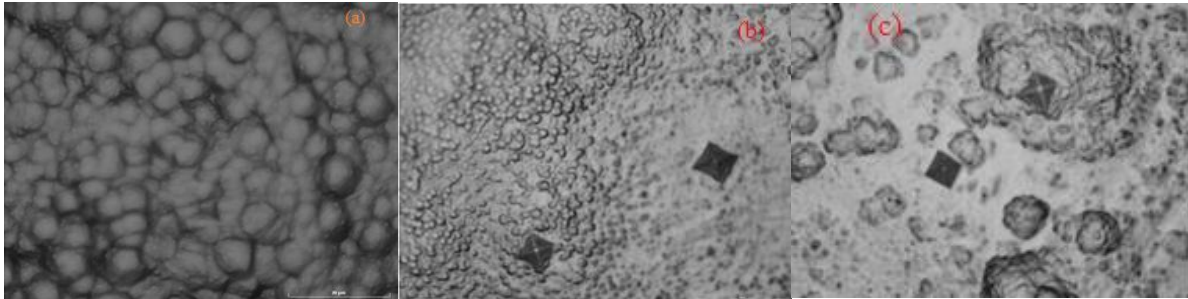


Fig. 4: Surface microstructure of Zircaloy-4 after irradiation. (a) Irradiated by 700 keV Cu ion 2.3 dpa. (b) and (c) Irradiated by 20 MeV Au ion at 4.5 dpa.

According to our experimental data, the hardness increases a little bit after irradiation for all ion species and energy. As example we presented in Fig.5 a and b respectively the evolution of the indenter imprint and the corresponding hardness in the case of sample irradiated by 20 MeV Au ion at 4.5 dpa. From Fig.4a one can see that the indenter imprint size decreases due to the irradiation induced-hardening. This increase in hardness in the irradiated region may come from irradiation induced damage or grain refinement structure.

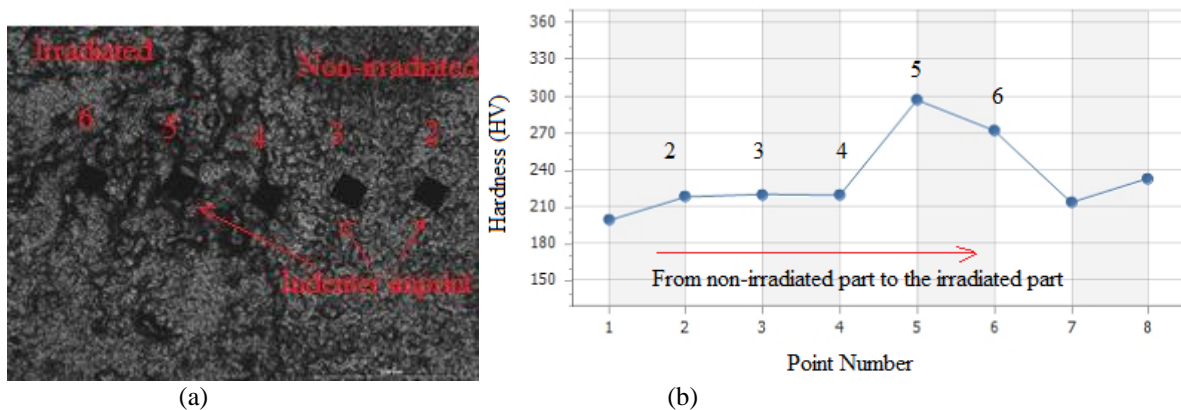


Fig. 5: (a) Optical microscopy micrograph of the sample irradiated with 20 MeV Au ion at 4.5 dpa showing the indenter imprint from the non-irradiated part to the irradiated part. (b) Hardness value evolution from the non-irradiated part to the irradiated part.

It is worth discussing the hardness value of the nanostructured zone. We measured the hardness of a few of the nanostructures observed after 20 MeV Au ions irradiation (see indenter imprint in Fig. 3 b and c) and found a large discrepancy between different parts of the same nanostructured area. The value vary between 200 HV and 300 HV indicating probably the formation of supersaturated solid solution [16].

4. Conclusion

In this communication, surface morphology evolution of zircaloy-4 under ion beam irradiation was presented. The result revealed the dependence of the microstructure formed on the ion beam species and energy. Fine grains with circular shape of 10 μm diameter were observed on zircaloy-4 surface irradiated with ion of low energy ($S_n/S_e \ll 1$). While the images showed eruption of the metal towards the surface with formation of nanostructure in the case of high energy ($S_n/S_e \gg 1$). In both case the ion beam induced surface degradation which affect the zircaloy-4 corrosion resistance.

Acknowledgements

The authors are indebted to the NCP accelerator staff for ion beam irradiation.

Funding Support

This research received no external funding.

Ethical Statement

This study does not contain any studies with human or animal subjects performed by any of the authors.

Conflict of Interest

The authors declare that they have no conflict of interest.

Data Availability Statement

Not applicable.

References

1. Jin HJ, Kim TK. Neutron irradiation performance of Zircaloy-4 under research reactor operating conditions. *Ann Nucl Energy*. 2015;75:309-15.
2. Arjhangmehr A, Fegghi SAH. Irradiation deformation near different atomic grain boundaries in α -Zr: An investigation of thermodynamics and kinetics of point defects. *Sci Rep*. 2016;6:23333. doi: 10.1038/srep23333.
3. Raquel ML, Arnaldo HPA. Influence of neutron irradiation on the stability of the precipitates in zircaloy- A critical review. In: *International Nuclear Atlantic Conference - INAC 2013*; 2013; Recife, PE, Brazil.
4. Adamson R, Griffiths M, Patterson C. Irradiation Growth of Zirconium Alloys: A Review. 2017. Advanced Nuclear Technology International, Tollerod, Sweden. Available from: https://www.antinternational.com/docs/samples/FM/04/ZIRAT22-IZNA17_Irradiation_Growth_of_Zirconium_Alloys_Sample.pdf
5. Buckley SN. Properties of Reactor Materials and the Effects of Irradiation Damage. London: Butterworths; 1961. p. 443. Buckley SN. Irradiation Growth in Properties of Reactor Materials and Effects on Radiation Damage. In: Littler DJ, editor. London: Butterworth; 1962. p. 413.
6. Kelly PM. Irradiation Growth in Zirconium. In: International Conference of Physical Metallurgy of Reactor Fuel Elements; 1973; *Berkeley Nuclear Laboratories*, UK.
7. Nichols EA. Radiation Enhanced Creep. In: Radiation Damage in Metals. Metals Park, OH: American Society for Metals; 1976. p. 267-94.
8. Li Y, Ghoniem N. Cluster dynamics modeling of irradiation growth in single crystal Zr. *J Nucl Mater*. 2020;540:152312.
9. Carpenter GJC, Murgatroyd RA, Rogerson A, Watters JF. Irradiation growth of zirconium single crystals. *J Nucl Mater*. 1988;101:28-37.
10. Rogerson A. Irradiation growth in annealed and 25% cold-worked zircaloy-2 between 353-673 K. *J Nucl Mater*. 1988;154:276-85.
11. Cazado ME, Goldberg E, Togneri MA, Denis A, Soba A. A new irradiation growth model for Zr-based components of nuclear reactors for the DIONISIO code. *Nucl Eng Des*. 2021;373:111009.
12. Cai J, Guan QF, Lv P, Zhang C, Yin Y. Crater Formation on the Surface of Pure Metal and Alloy Irradiated by High Current Pulsed Electron Beam. *High Temp Mater Proc*. 2018;37(8):777-84.
13. Ziegler JF, Biersack JP, Littmark U. The Stopping and Range of Ions in Solids. New York: Pergamon; 1985. Available from: <http://srim.org/>
14. Hengstler-Eger RM, Baldo P, Beck L, Dorner J, Ertl K, Hoffmann PB, et al. Heavy ion irradiation induced dislocation loops in AREVA's M5Ö alloy. *J Nucl Mater*. 2012;423:170-82.
15. Adamson RB, Coleman CE, Griffiths M. Irradiation creep and growth of zirconium alloys: A critical review. *J Nucl Mater*. 2019;521:167-244.
16. Han ZY, Ji L, Cai, Zou H, Wang ZP, Guan QF. Surface Nanocrystallization of 3Cr13 Stainless Steel Induced by High-Current Pulsed Electron Beam Irradiation. *J Nanomater*. 2013;603586:603586.